

The effects of adipose-derived stem cell transplantation on tendon-bone healing in a model of chronic rotator cuff tear with suprascapular nerve injury

Kenichiro Eshima

Kurume University Hospital

Hiroki Ohzono (✉ ohzono_hiroki@med.kurume-u.ac.jp)

Kurume University Medical Center

Masafumi Gotoh

Kurume University Medical Center

Hidehiro Nakamura

Kurume University Medical Center

Takahiro Okawa

Kurume University Medical Center

Naoto Shiba

Kurume University Hospital

Research Article

Keywords: suprascapular nerve injury, bone-tendon interface healing, rotator cuff tear, adipose-derived stem cells, animal model

Posted Date: September 21st, 2022

DOI: <https://doi.org/10.21203/rs.3.rs-1906166/v2>

License:  This work is licensed under a Creative Commons Attribution 4.0 International License.

[Read Full License](#)

Abstract

Background: Recurrence of massive rotator cuff tears (RCTs) are relatively common due to resultant muscle atrophy and fatty infiltration, possibly caused by scapular nerve (SN) injury. Growing evidence suggests that adipose-derived stem cells (ADSCs) are useful tools for regeneration in chronic RCT models. However, data on the effects of ADSCs on in chronic RCT models with SNI are limited. This study aimed to investigate the effect of ADSCs on tendon-bone healing in a chronic rotator cuff tear (RCT) model with scapular nerve (SN) injury.

Methods: Overall, 36 adult rats (weight=344±33 g) were equally divided into the ADSC (+) and ADSC (-) group. Both groups underwent right shoulder surgery in which the supraspinatus was detached, and SN injury was induced; the untreated left shoulder in the ADSC (-) group was used as a control. In the ADSC (+) group, abdominal fat was collected to culture ADSCs. At 6 weeks postoperatively, the ADSC (+) group underwent surgical tendon repair with ADSC injection, whereas the ADSC (-) group underwent tendon repair with saline injection. Shoulders were harvested at 10, 14, and 18 weeks and underwent histological, fluorescent, and biomechanical analyses.

Results: In bone-tendon junction, a firm enthesis, including dense mature fibrocartilage and well-aligned cells, was observed in the ADSC (+) group. Conversely, decreased cell density and immature fibrocartilage were observed in the ADSC (-) group. Fatty infiltration was more uncommon in the ADSC (+) group compared to that in the ADSC (-) group. The mean maximum stress and linear stiffness was higher in the ADSC (+) group than in the ADSC (-) group at 18 weeks. Neither the mean Young's modulus nor the cross-sectional area were significantly different throughout the study.

Conclusion: ADSC injection produced better histological and biomechanical outcomes. Thus, ADSC supplementation showed a positive effect on tendon-bone healing in a chronic RCT model with SN injury; therefore, ADSC injection possibly accelerates recovery in large RCT repair.

Background

Arthroscopic rotator cuff repair (ARCR) mostly produces acceptable clinical outcomes.¹⁷ However, ARCR in chronic massive rotator cuff tears (RCTs) remains challenging, with a high structural failure rate between 34% and 94%.⁴ Ladermann *et al.* have reported that recurrence rates of massive RCTs are as high as 80% because of tendon retraction, muscle atrophy, fatty infiltration, and osteoporosis.¹⁴ Additionally, Choi *et al.* have reported that recurrence rates of massive RCTs were 53.3% (8/15 patients), which was significantly more common in patients with preoperative fatty degeneration.²

Previous studies have indicated a significant association between suprascapular nerve (SN) injuries and rotator cuff (RC) muscle fatty degeneration in the high recurrence rates of massive RCTs.²²⁻²⁶ Mallon *et al.* reported that all patients presenting with massive cuff tears (n = 8) had SN neuropathy in the supraspinatus (SSP) and/or infraspinatus (ISP) muscles, as shown by electromyography analysis.¹⁶

Albritton *et al.* reported that the degree of RC muscle atrophy frequently observed after a massive tear may be explained by increased tension on the nerve due to muscle retraction in freshly frozen cadavers.¹ Large or massive RCTs cause the SN tract to become strangulated. SN injury subsequently causes atrophy and fat infiltration of the RC, which results in a lack of healing at the repair site.

Mesenchymal stem cells (MSCs) are commonly used in tissue engineering for the treatment of various diseases. Among the beneficial effects of MSCs is that they can be readily isolated from autologous tissues.²⁷ Jo *et al.* evaluated the safety and efficacy of an intra-tendinous injection of adipose-derived stem cells (ADSCs) for the treatment of partial-thickness RCTs and showed that no treatment-related adverse events occurred at a 2-year follow-up.¹⁰ The intra-tendinous injection of ADSCs reduced shoulder pain by approximately 90% at 1 and 2 years in the mid- and high-dose groups. Additionally, the strength of the SSP, ISP, and teres minor increased by greater than 50% at 2 years post-injection in the high-dose group. Pauyo *et al.* reported on the effect of ADSCs on healing of a chronic massive RCT rodent model and showed that ADSCs may have a greater effect on chronic tears, as shown by improvements in bone morphometric parameters.¹⁹ In that study, patients treated with ADSCs showed significant clinical improvements compared to patients treated with corticosteroid injection at 6 and 12 months post-treatment.

MSCs have the potential to become a variety of adult tissue cells, including tenocytes, chondrocytes, and osteoblasts.⁹ Additionally, they are a source of multiple growth factors that aid in the establishment of an environment conducive to soft and hard tissue generation. Recently, ADSCs have become increasingly used due to their minimal damage, low cost, and ubiquity. Furthermore, they can be isolated from various tissues, including bone marrow, the umbilical cord, and the placenta.¹⁵ In the field of RC surgery, basic studies have begun to evaluate the effects of ADSCs on RC regeneration.⁹

SN injury due to massive tears is closely associated with the development of fatty degeneration and/or muscle atrophy.²⁵ The chronic RCT model has been used in previous studies; however, none have used chronic tear models accompanied with nerve injury. In this study, we established a rodent model of chronic RCT repair with SN injury, mimicking a clinical setting. We hypothesized that the administration of ADSCs could decrease fatty infiltration and enhance tendon-bone healing in this model. The aim of this study was to evaluate the efficacy of ADSC injection for regenerating chronic RCTs.

Materials And Methods

All efforts were made to minimize the number of animals used and minimize the suffering of all animals.

Experimental design

A total of 36 adult male Sprague-Dawley rats (mean body weight: 344 ± 19 g) were divided into two groups: the ADSC (+) (n = 18) and ADSC (-) (n = 18) groups. Both groups underwent massive SSP detachment in the right shoulder, and the untreated left shoulder in the ADSC (-) group was used as a

control. To establish a chronic tendon tear, a thermo-setting polyurethane moldable resin was placed between the tendon edge and the tendon footprint. SN injury was achieved by applying a vascular clip for 20 s (clipping power 120 g/mm²).³ Additionally, the ADSC (+) group underwent abdominal operation to collect fat tissue for cell expansion.

Six weeks after surgery, the ADSC (+) group underwent tendon repair treatment with ADSC injection, and the ADSC (-) group underwent tendon repair treatment with saline injection. At 10, 14, and 18 weeks post-operation, the specimens were harvested and subjected to histological analysis, immunofluorescent staining, and mechanical testing. Details are summarized in Figure 1 and Figure 2.

Isolation of MSCs

Abdominal and inguinal fat was collected from the ADSC (+) group and washed with 1× phosphate-buffered saline (PBS). This fat was minced using scissors and subsequently placed in a 50-mL conical tube containing 40 ml of Dulbecco's modified Eagle's medium (DMEM) supplemented with 0.075% collagenase type 1 and 2% penicillin/streptomycin. The fat was digested in a shaker for 1 h at 37°C, and the digest was passed through a 70-µm filter. The solution was centrifuged at 500 g for 5 min, and the pellets were washed with PBS twice. The resulting pellet was resuspended and expanded in DMEM with 10% fetal bovine serum in T300 tissue culture flasks at 37°C in a humidified atmosphere containing 5% CO₂. Semi-confluent MSCs from passage 2 to 5 were used for subsequent experiments. Confluent MSCs were used for implantation, and the concentration used was 3.78×10⁷ cells.

Surgical procedure

All rats were treated according to the guidelines of the Institutional Animal Care and Use Committee. They were anesthetized with isoflurane at a high oxygen flow rate. A middle longitudinal skin incision was made, and the subcutaneous tissue was divided to expose the deltoid. After exposure of the SSP tendon, the tendon insertion was detached and resected using a #11 scalpel blade, and the cartilaginous portion was protected at its insertion. The SN was pinched by the vascular clip for 20 s (clipping power 120 g/mm²) just anterior to the suprascapular notch. After the deltoid muscle incision was closed, the ADSC pellet was injected at the repair site using an 18G needle. The wound was then closed at each layer, and the animals were allowed to move freely in their cages after the operation. The surgical protocol was similar to that described in a previous report.¹²

Histological analysis

Axial sections of 5-µm thickness at the muscle belly (SSP) were processed from frozen sections and stained with hematoxylin and eosin and oil red. To observe fatty tissue, fixed specimens were frozen briefly with iced 99.5% ethanol and cut axially into 10-µm-thick sections. The specimens were visualized under a light microscope (BZ-X710; Keyence, Osaka, Japan), and photomicrographs were obtained.

Muscle atrophy was identified by a few suggestive findings, such as an angular shape of muscle fibers rather than a round shape, decreased distance between myonuclei, and centralization of myonuclei. The muscle fiber size was not measured.

Immunofluorescence staining

Fatty infiltration was identified using Perilipin's methods. Muscle belly samples were fixed, embedded in paraffin, and sectioned at a thickness of 5 μm . Sections were stained with a guinea pig anti-perilipin antibody, followed by staining with a goat anti-guinea pig Alexa Fluor 488 secondary antibody. The sections were examined via fluorescence.

Mechanical testing at the tendon-bone insertion

All biomechanical testing specimens were dissected, stored at -80°C , and thawed the day before biomechanical testing. Except for the SSP tendon-humerus complex, soft tissues over the humerus were removed. The SSP tendon was secured to a screw grip using sandpaper and ethyl cyanoacrylate. Specimens in saline were subjected to micro-CT (R-mCT2; Rigaku Corporation, Tokyo, Japan) on the day of testing. Each sample was placed in a holder and scanned at 90 kV and 160 μA . Following micro-CT scanning, the specimens were placed in a tensile testing machine (TENSILON RTE-1210; Orientec, Tokyo, Japan). The humerus was secured to a custom-designed pod using a capping compound. The SSP tendon-humerus complex was positioned to allow tensile loading in the longitudinal direction of the SSP tendon-humerus interface. The specimens were preloaded to 0.1 N for 5 min, followed by five cycles of loading and unloading at a cross-head speed of 5 mm/min. Samples were then loaded to failure at a rate of 1 mm/min, and mechanical properties were calculated. Failure modes were recorded for each specimen. The linear stiffness was calculated by determining the slope of the linear portion of the load-elongation curve. The ultimate stress was calculated by dividing the ultimate load-to-failure by the cross-sectional area of the repaired tendon-bone interface, obtained from the axial section of the micro-CT image. Young's modulus was calculated by determining the slope of the linear portion of the stress-strain curve. The strain was calculated by dividing the elongation by the initial length obtained from the coronal section of the micro-CT image. This testing protocol was similar to that described previously.¹²

Statistical analysis

Statistical analysis was performed using JMP version 16 (SAS Institute Inc., Cary, NC, USA). A Mann-Whitney test was used to compare the ADSC (+) vs. ADSC (-) group, the ADSC (+) vs. control group, and the ADSC (-) vs. control group at each time point by comparing the mechanical properties. Then, the Holm-Bonferroni sequential correction method was used to adjust the p values for multiple comparisons. Data are expressed as the mean \pm standard deviation. Statistical significance was set at $p < 0.05$.

Results

Histological observation of the muscle belly and enthesis

In the ADSC (+) group, muscle fibers were slightly atrophic, with a regular nuclear arrangement. These changes were similar throughout the experimental period. In contrast, in the ADSC (-) group, the muscle fibers showed more advanced atrophy with irregular nuclear arrangement, and the changes became more prominent over the experimental period (Figure 3).

Histology at the tendon-bone insertion

The tendon-bone junction was reconstructed using granulated tissue in both groups. A firm enthesis was observed in the ADSC (+) group, including dense mature fibrocartilage and well-aligned cells. In the ADSC (-) group, the enthesis had a relatively decreased cell density and immature fibrocartilage (Figure 4).

Immunofluorescence staining

At week 18, there was some fatty infiltration at the muscle belly in the ADSC (-) group. Conversely, lower fatty infiltration was found in the ADSC (+) and control groups (Figure 5).

Biomechanical testing

The mean maximum stress in the control, ADSC (+), and ADSC (-) groups were 3.47/1.40/1.02 N/m² at 10 weeks, 3.21/1.79/0.81 N/m² at 14 weeks, and 2.87/2.64/0.87 N/m² at 18 weeks, respectively. There was a significant difference between the ADSC (+) and ADSC (-) group at both 14 and 18 weeks. The linear stiffness was 61.3/23.5/21.5 N/mm at 10 weeks, 44.2 /28.8 /22.0 N/mm at 14 weeks, and 38.0/30.4/16.0 N/mm at 18 weeks, respectively. There was a significant difference between the ADSC (+) and ADSC (-) groups at 18 weeks. The mean Young's modulus was 11.3/2.11/1.99 MPa at 10 weeks, 7.21/2.19/1.56 MPa at 14 weeks, and 5.93/3.53/1.48 MPa at 18 weeks, respectively. There was no significant difference between the ADSC (+) and ADSC (-) groups. The cross-sectional area was 9.20/25.5/28.1 mm² at 10 weeks, 14.0/28.2/35.2 mm² at 14 weeks, 15.7/ 39.5 /21.0 mm² at 18 weeks, respectively. There was no significant difference between the ADSC (+) and ADSC (-) groups (Figure 6).

Discussion

Compared to other sources, adipose tissue is a useful stem cell source because of its accessibility, abundance, and less painful collection procedure. ADSCs can be maintained and expanded in tissue culture for long periods without losing their differentiation capacity, leading to large cell quantities.⁶ A systematic review reported on the therapeutic advantages of ADSCs in comparison to bone marrow and umbilical cord-derived MSCs.¹⁵ Indeed, ADSCs have shown significant chondrogenic potential for use in tissue engineering. These cells are now widely accepted for use in bone and cartilage regeneration and repair. Thus, a notable finding of this study was that in the chronic RCT model with SN injury, ADSC transplantation improved tendon-bone healing, as well as fatty degeneration and atrophy in the involved

muscles. This led to enhanced biomechanical properties and granulation maturity at the repair site. To our knowledge, no such studies have been published thus far.

In clinical settings, the re-tear rates of massive RCT are as high as 80%¹⁴ due to tendon retraction, muscle atrophy and fatty infiltration. Several researchers have reported a relationship between SN injury and RCTs.^{22 5} In fresh-frozen cadavers, the degree of RC muscle atrophy observed after a massive tear was explained by increased tension on the nerve due to muscle retraction.¹ In large or massive RCTs, tract-strangulated SN injury causes atrophy and fat infiltration of the RC muscle and a lack of healing at the repair site.¹³ In the present study, we established a chronic RCT model with SN injury pinched by the vascular clip to mimic the clinical setting and then examined the effects of ADSC transplantation on the repaired enthesis in this model.

Benjamin *et al.* have also examined the effect of ADSCs on the healing of chronic massive RCTs.²¹ In their model, SSP transection and intramuscular botulinum toxin injection were performed, and 8 weeks after index surgery, surgical repair was supplemented with ADSCs + fibrin, gelatin methacrylate, or TGF- β 3. They found no significant difference among any groups at 4 weeks after the delayed repair.²¹ In a chronic RCT rabbit model, Oh *et al.* performed 1) repair only, 2) repair + ADSCs, 3) ADSCs only, or 4) repair + saline 6 weeks after they cut the SSC for the index procedure. There were no significant differences in the biomechanical testing between the ADSC + repair and repair + saline groups, although the average load-to-failure of the ADSC + repair group was higher than that of the saline + repair group. They concluded that the negative effect of ADSCs may be attributed to a single time point observation (4 to 6 weeks after delayed repair).¹⁸ In the present study, the effects of ADSCs on the repaired enthesis became clear at 8 weeks or more after delayed repair. These results indicate that a longer observational period is needed to confirm the effect of ADSC transplantation on delay-repaired enthesis in chronic RCT models.

Kaizawa *et al.* compared the effects of ADSCs (4×10^6 cells) with or without scaffold on tendon healing, but no apparent advantage of scaffold use was observed.¹¹ Rak Kwon *et al.* evaluated the efficacy of MSCs (1M cells) with three-dimensional bio-printed scaffolds for regeneration in a chronic RCT rabbit model and concluded that there was no significant difference in the gross tear size between patients with and without scaffolds. Thus, previous studies have consistently failed to confirm the advantage of scaffold use in chronic cuff repair models.²⁰

Jo *et al.* reported that in a dose-escalation human clinical trial, the amount of ADSCs administered is an important factor in regenerating the RC and that intra-tendinous ADSC injection without scaffolds reduced shoulder pain by approximately 90% and muscle strength increased by greater than 50%.¹⁰ Shoulder function measured with six commonly used scores improved for up to 2 years in all dose groups. Structural outcomes evaluated with magnetic resonance imaging showed that the volume of bursal-sided defects in the high-dose group nearly disappeared at 1 year and did not recur for up to 2 years. In the present study, ADSCs were directly injected at 2–40 times the concentration in previous reports using MSCs with scaffolds.^{20 7,21} Moreover, ADSCs were injected after the deltoid suture to

reduce outflow loss. Consequently, in terms of biomechanical testing and histological aspects, we confirmed better results in the ADSC (+) group than in the ADSC (-) group.

Although our results successfully indicate the effects of ADSC injection without a scaffold in a chronic cuff repair model, several reports have shown a high initial cell loss (approximately 75%) over 24 h after MSC injection without a scaffold.²³ As described above, in previous studies that examined the effects of ADSC injection with scaffolds, no apparent effect was observed because of the insufficient number of ADSCs used. The resolution of these issues remains to be elucidated in future studies.

The conditions of the RC parenchyma, enthesis, and nerve are the major factors influencing postoperative prognosis in RCTs. Specifically, impaired condition of the SN compromises the RC enthesis structure. In a rodent model with SN transection, Gereli *et al.* demonstrated that SN injury impaired the enthesis by reducing cellularity at all enthesal zones and diminished the collagen bundle in the tendon zone.⁵ Sun *et al.* evaluated the histomorphology of the fibrocartilage area of bone-tendon junction formation in a rodent model and reported that there was less cellularity and cell maturity in the group with SN transection.²⁵ The present study showed that regenerated enthesis with SN injury was relatively more mature in the ADSC (+) group compared to that in the ADSC (-) group, with significant improvements in both biomechanical and histological parameters. We postulate the following two possibilities: ADSCs lead to enthesis healing and then, transmission of suitable biomechanical stimulation via this healed enthesis secondarily caused recovery of the damaged nerve and muscles; alternatively, ADSCs lead to enthesis healing, and extra-articular recruitment of ADSCs to the SN simultaneously improved this damaged nerve. The detailed mechanisms by which ADSCs lead to improvements in enthesis repair following SN injury are subjects of ongoing research in our laboratory.

Some limitations of the current study should be acknowledged. First, the anatomy and function of the rat shoulder differs from those of the human shoulder. In particular, the acromial arch in quadrupedal animals is different because it involves reduced coverage of the subscapularis compared to bipedal animals.⁸ However, the anatomy of the rat is more similar to that of the human shoulder joint.²⁴ Second, ADSCs were not labeled, which would have permitted the analysis of cell retention at the healing site over time.

Conclusion

We evaluated the effect of ADSCs on the repair site in a chronic RCT model with SN injury. The ADSC (+) group exhibited better results than the ADSC (-) group in terms of mechanical and histological parameters. In addition, in the ADSC (+) group, the repaired enthesis had better fibrocartilage maturity with increased cell density, and the muscle fibers showed less atrophy in this group. Thus, ADSC treatment has a positive effect on the tendon-bone healing in a chronic RCT model with SN injury.

Abbreviations

ADSC	Adipose-derived stem cell
ARCR	Arthroscopic rotator cuff repair
DMEM	Dulbecco's modified Eagle's medium
ISP	Infraspinatus
MSC	Mesenchymal stem cells
PBS	Phosphate-buffered saline
RC	Rotator cuff
RCT	Rotator cuff tears
SN	Scapular nerve
SSP	Supraspinatus

Declarations

Ethics Approval: This study was conducted in accordance with the National Institute of Health Guidelines for Animal Research and was approved by the Animal Studies and Institutional Animal Care and Use Committees of our institution (#2020-134) and was approved by the Ethics Review Board of the Animal Care Centre in our institute (#2021-118).

Consent for publication: Not applicable

Availability of data and materials

Conflicts of interest: The Authors declare that there is no conflict of interest.

Funding: This research received grant from Aid in Scientific Research.

Acknowledgments: None.

Authors' contributions

All authors (1) made substantial contributions to the study concept or the data analysis or interpretation; (2) drafted the manuscript or revised it critically for important intellectual content; (3) approved the final version of the manuscript to be published; and (4) agreed to be accountable for all aspects of the work.

References

1. Albritton MJ, Graham RD, Richards RS, Basamania CJ. An anatomic study of the effects on the suprascapular nerve due to retraction of the supraspinatus muscle after a rotator cuff tear. *Journal of Shoulder and Elbow Surgery*. 2003;12(5):497-500.
2. Choi S, Kim MK, Kim GM, et al. Factors associated with clinical and structural outcomes after arthroscopic rotator cuff repair with a suture bridge technique in medium, large, and massive tears. *J Shoulder Elbow Surg*. 2014;23(11):1675-1681.
3. Farinas AF, Manzanera Esteve IV, Pollins AC, et al. Diffusion Magnetic Resonance Imaging Predicts Peripheral Nerve Recovery in a Rat Sciatic Nerve Injury Model. *Plast Reconstr Surg*. 2020;145(4):949-956.
4. Galatz LM, Ball CM, Teefey SA, Middleton WD, Yamaguchi K. The outcome and repair integrity of completely arthroscopically repaired large and massive rotator cuff tears. *J Bone Joint Surg Am*. 2004;86(2):219-224.
5. Gereli A, Uslu S, Okur B, et al. Effect of suprascapular nerve injury on rotator cuff enthesis. *J Shoulder Elbow Surg*. 2020;29(8):1584-1589.
6. Goldenberg BT, Lacheta L, Dekker TJ, et al. Biologics to Improve Healing in Large and Massive Rotator Cuff Tears: A Critical Review. *Orthop Res Rev*. 2020;12:151-160.
7. Gulotta LV, Kovacevic D, Ehteshami JR, et al. Application of Bone Marrow-Derived Mesenchymal Stem Cells in a Rotator Cuff Repair Model. *The American Journal of Sports Medicine*. 2009;37(11):2126-2133.
8. Gupta R, Lee TQ. Contributions of the different rabbit models to our understanding of rotator cuff pathology. *J Shoulder Elbow Surg*. 2007;16(5 Suppl):S149-157.
9. Hernigou P, Flouzat Lachaniette CH, Delambre J, et al. Biologic augmentation of rotator cuff repair with mesenchymal stem cells during arthroscopy improves healing and prevents further tears: a case-controlled study. *Int Orthop*. 2014;38(9):1811-1818.
10. Jo CH, Chai JW, Jeong EC, et al. Intratendinous Injection of Autologous Adipose Tissue-Derived Mesenchymal Stem Cells for the Treatment of Rotator Cuff Disease: A First-In-Human Trial. *Stem Cells*. 2018;36(9):1441-1450.
11. Kaizawa Y, Franklin A, Leyden J, et al. Augmentation of chronic rotator cuff healing using adipose-derived stem cell-seeded human tendon-derived hydrogel. *J Orthop Res*. 2019;37(4):877-886.
12. Kanazawa T, Gotoh M, Ohta K, et al. Histomorphometric and ultrastructural analysis of the tendon-bone interface after rotator cuff repair in a rat model. *Sci Rep*. 2016;6:33800.
13. Kim HM, Galatz LM, Lim C, Havlioglu N, Thomopoulos S. The effect of tear size and nerve injury on rotator cuff muscle fatty degeneration in a rodent animal model. *J Shoulder Elbow Surg*. 2012;21(7):847-858.
14. Ladermann A, Denard PJ, Collin P. Massive rotator cuff tears: definition and treatment. *Int Orthop*. 2015;39(12):2403-2414.
15. Lavorato A, Raimondo S, Boido M, et al. Mesenchymal Stem Cell Treatment Perspectives in Peripheral Nerve Regeneration: Systematic Review. *Int J Mol Sci*. 2021;22(2).

16. Mallon WJ, Wilson RJ, Basamania CJ. The association of suprascapular neuropathy with massive rotator cuff tears: a preliminary report. *J Shoulder Elbow Surg.* 2006;15(4):395-398.
17. McElvany MD, McGoldrick E, Gee AO, Neradilek MB, Matsen FA, 3rd. Rotator cuff repair: published evidence on factors associated with repair integrity and clinical outcome. *Am J Sports Med.* 2015;43(2):491-500.
18. Oh JH, Chung SW, Kim SH, Chung JY, Kim JY. 2013 Neer Award: Effect of the adipose-derived stem cell for the improvement of fatty degeneration and rotator cuff healing in rabbit model. *J Shoulder Elbow Surg.* 2014;23(4):445-455.
19. Pauyo T, Rothrauff BB, Chao T, et al. The Effect of Adipose-derived Mesenchymal Stem Cells on Healing of Massive Chronic Rotator Cuff Tear in Rodent Model. *Orthopaedic Journal of Sports Medicine.* 2017;5(7_suppl6).
20. Rak Kwon D, Jung S, Jang J, et al. A 3-Dimensional Bioprinted Scaffold With Human Umbilical Cord Blood-Mesenchymal Stem Cells Improves Regeneration of Chronic Full-Thickness Rotator Cuff Tear in a Rabbit Model. *Am J Sports Med.* 2020;48(4):947-958.
21. Rothrauff BB, Smith CA, Ferrer GA, et al. The effect of adipose-derived stem cells on enthesis healing after repair of acute and chronic massive rotator cuff tears in rats. *J Shoulder Elbow Surg.* 2019;28(4):654-664.
22. Sasaki Y, Ochiai N, Hashimoto E, et al. Relationship between neuropathy proximal to the suprascapular nerve and rotator cuff tear in a rodent model. *J Orthop Sci.* 2018;23(2):414-419.
23. Smith RK, Werling NJ, Dakin SG, et al. Beneficial effects of autologous bone marrow-derived mesenchymal stem cells in naturally occurring tendinopathy. *PLoS One.* 2013;8(9):e75697.
24. Soslowsky LJ, Carpenter JE, DeBano CM, Banerji I, Moalli MR. Development and use of an animal model for investigations on rotator cuff disease. *Journal of Shoulder and Elbow Surgery.* 1996;5(5):383-392.
25. Sun Y, Wang C, Kwak JM, et al. Suprascapular nerve neuropathy leads to supraspinatus tendon degeneration. *J Orthop Sci.* 2020;25(4):588-594.
26. Wang Z, Feeley BT, Kim HT, Liu X. Reversal of Fatty Infiltration After Suprascapular Nerve Compression Release Is Dependent on UCP1 Expression in Mice. *Clin Orthop Relat Res.* 2018;476(8):1665-1679.
27. Xie Q, Liu R, Jiang J, et al. What is the impact of human umbilical cord mesenchymal stem cell transplantation on clinical treatment? *Stem Cell Res Ther.* 2020;11(1):519.

Figures

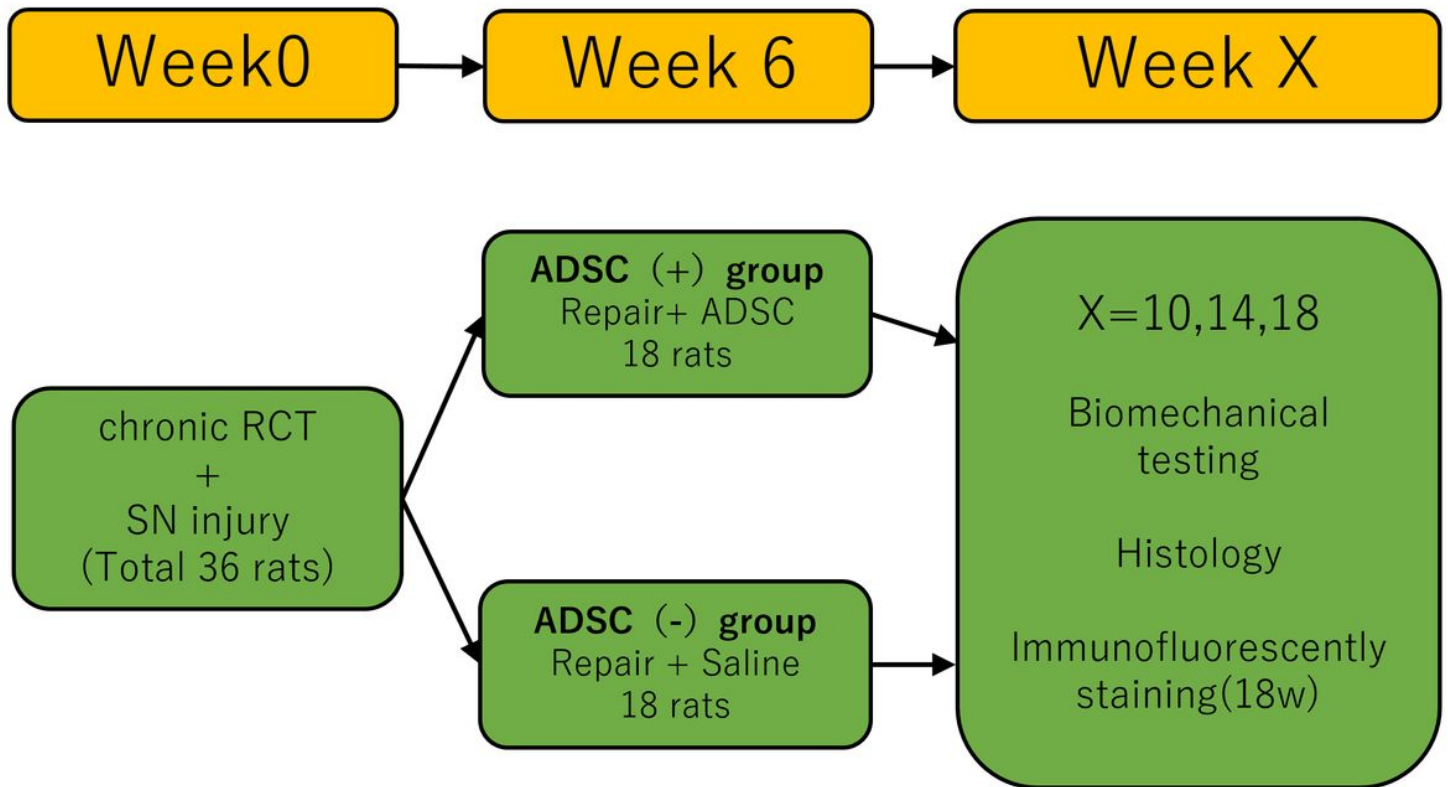


Figure 1

RCT: rotator cuff tear, SN: scapular nerve, ADSC: adipose-derived stem cell

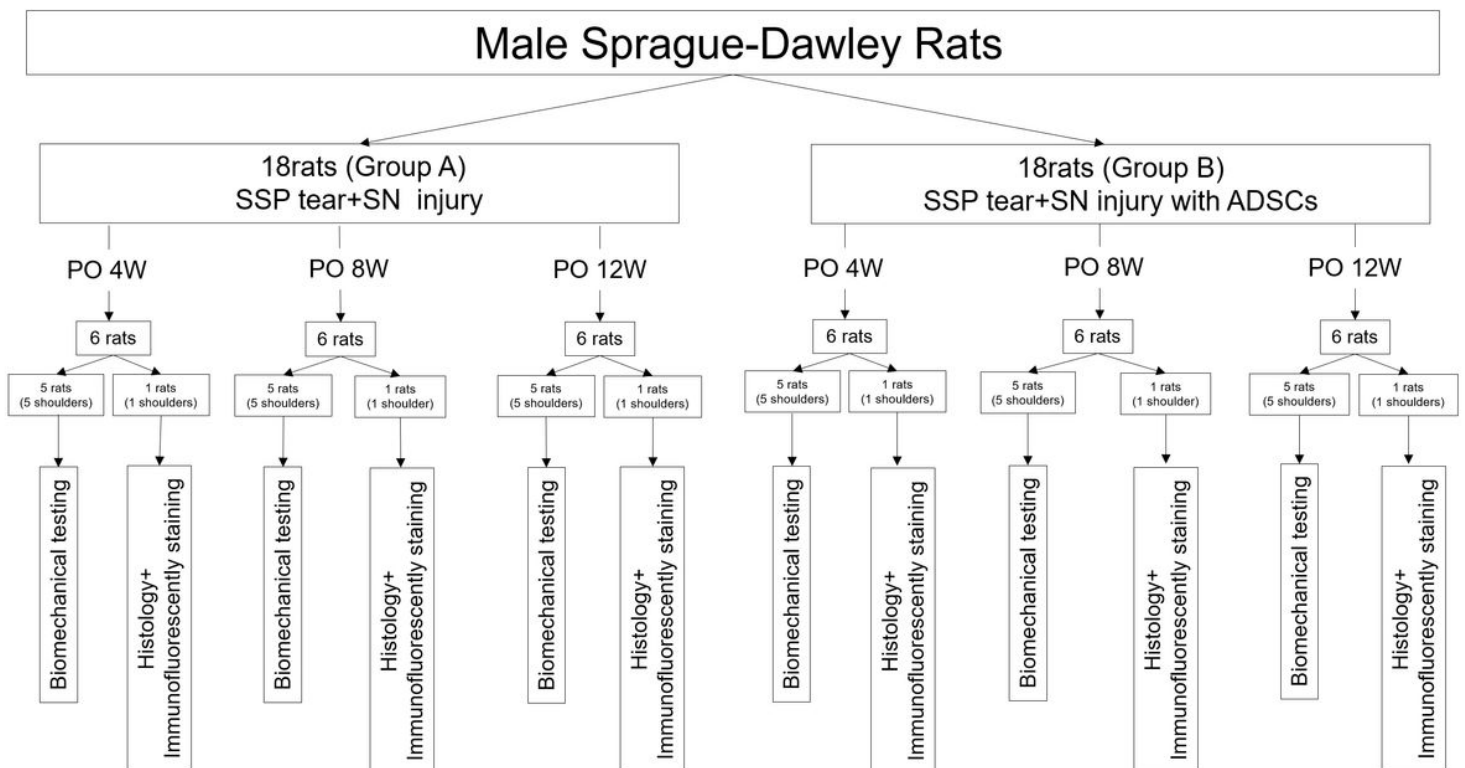


Figure 2

Flow diagram of the study design, illustrating how the rats were divided into groups for the three time points. SSP: supraspinatus, PO: postoperative, SN: suprascapular nerve

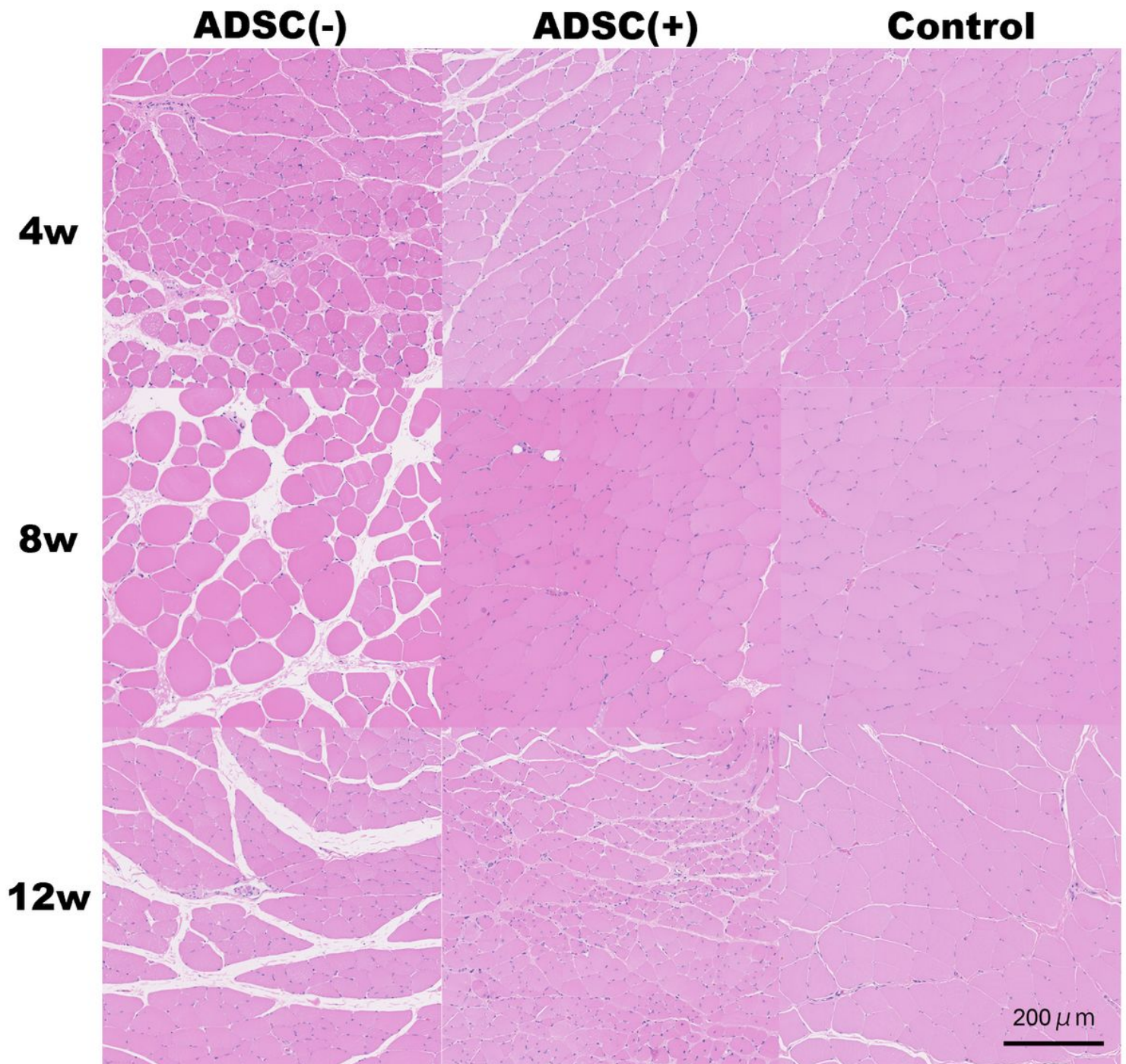


Figure 3

Histological findings (hematoxylin and eosin stain). ADSC: adipose-derived stem cell

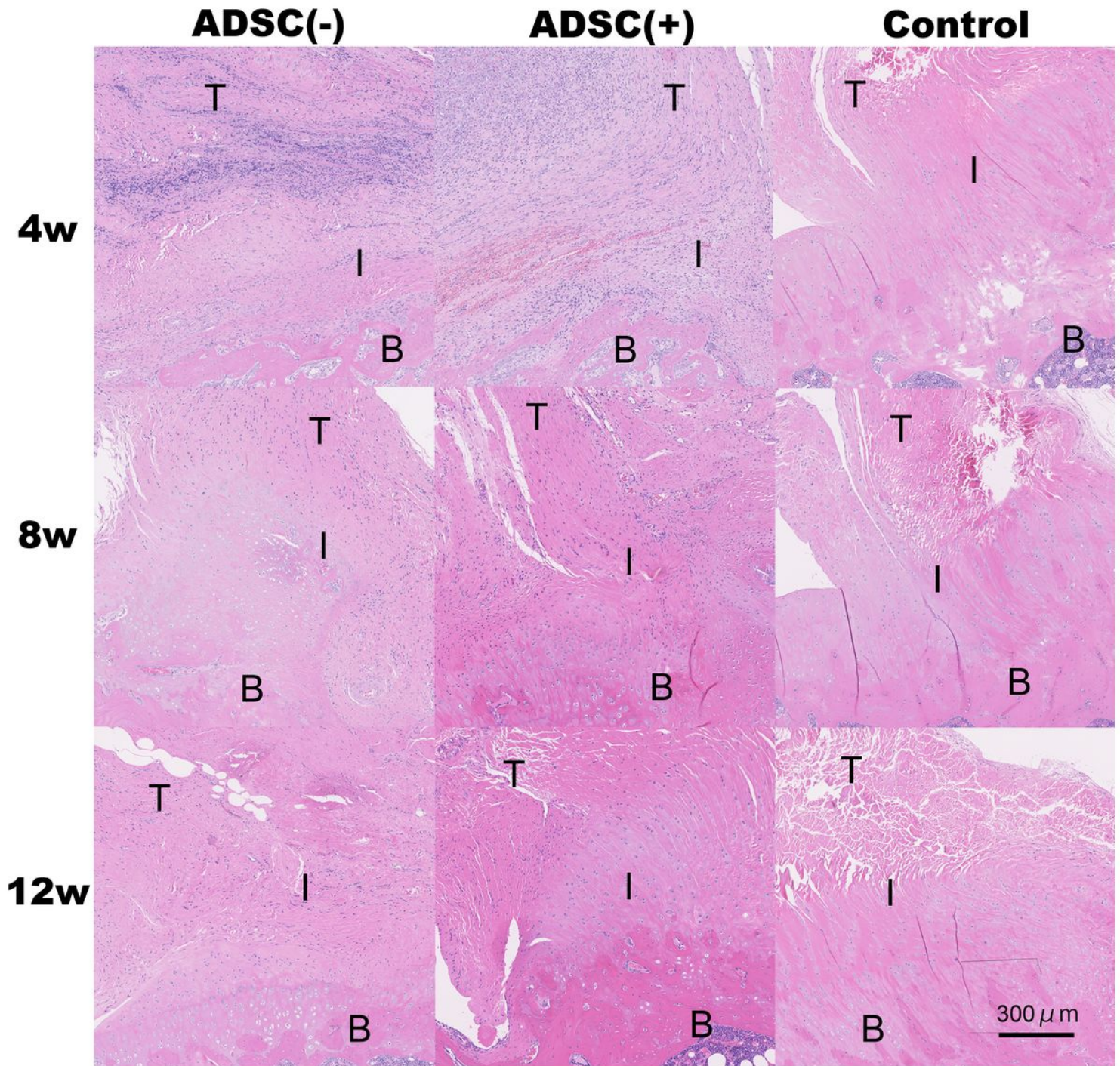


Figure 4

Histological findings (hematoxylin and eosin stain).

ADSC: adipose-derived stem cell, T: tendon, B: bone, I: tendon-bone interface

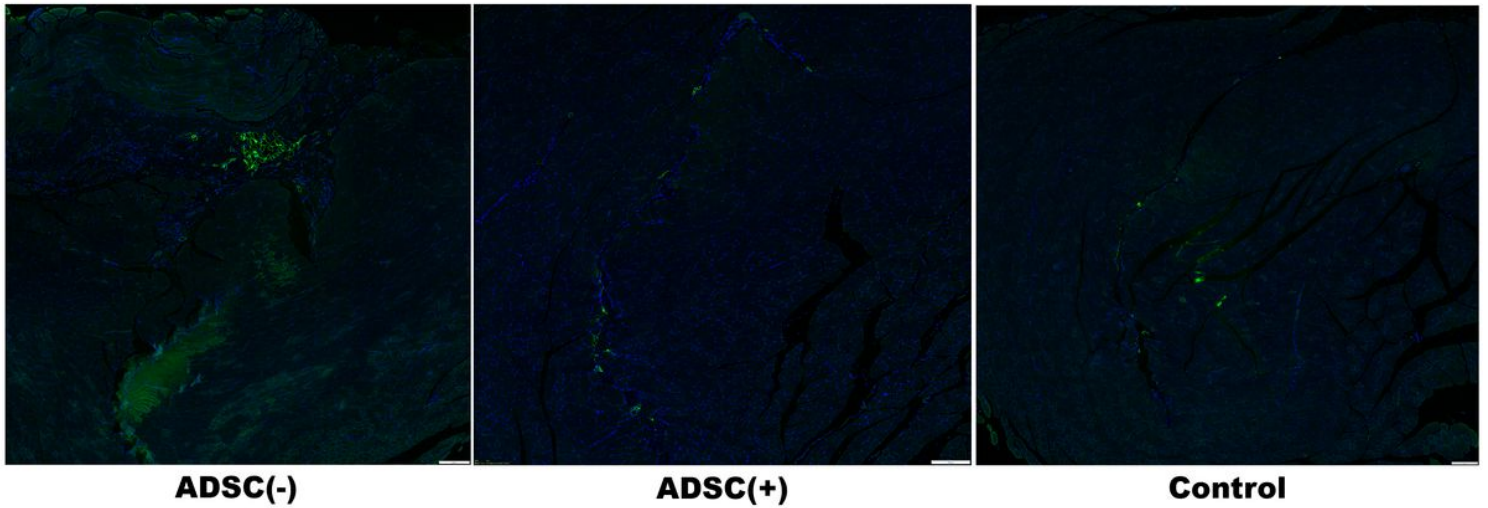


Figure 5

Immunofluorescence staining of the muscle belly at 18 weeks. ADSC: adipose-derived stem cell

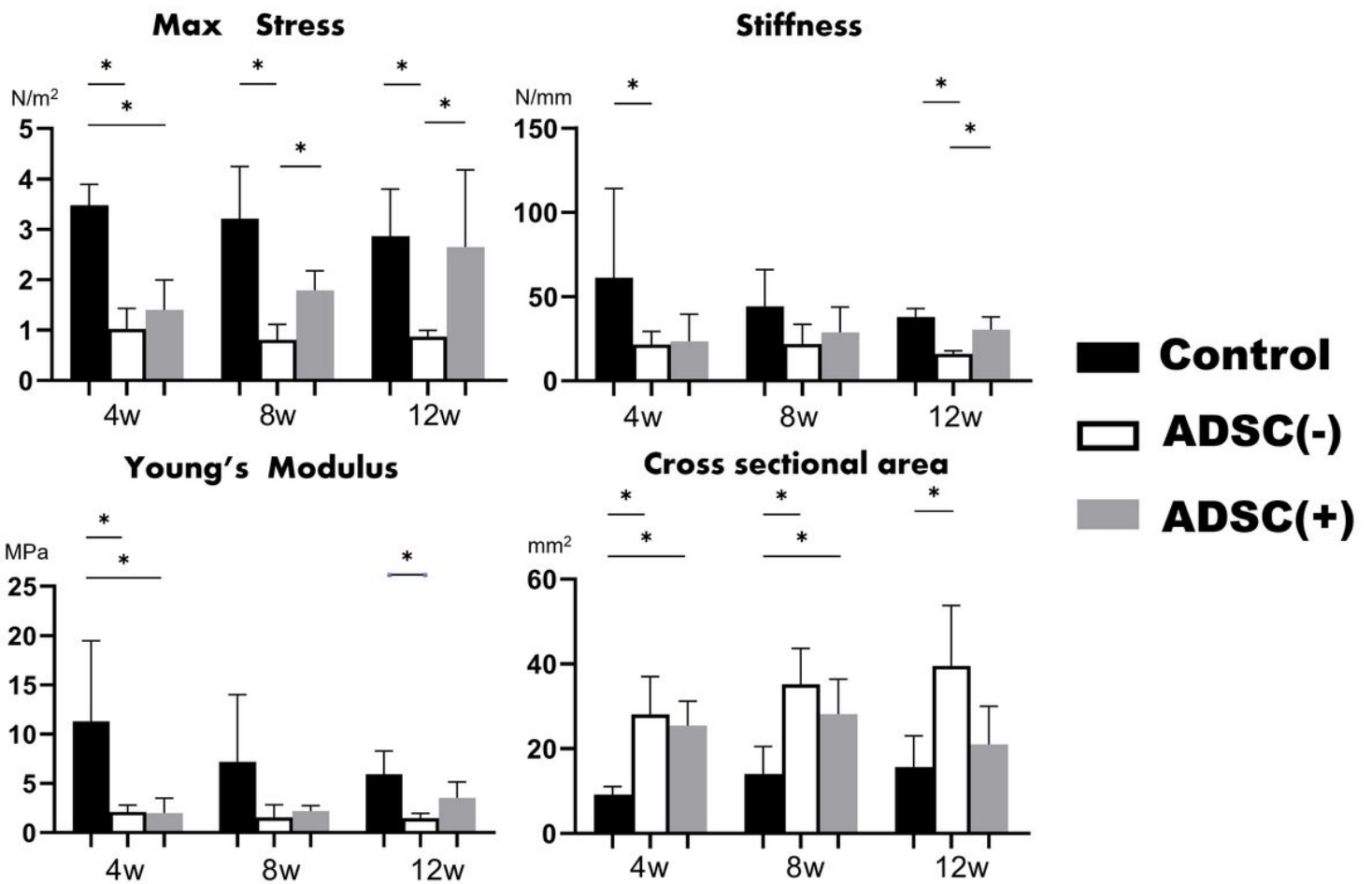


Figure 6

The results of biomechanical testing; there were significant difference between ADSC(+) group and ADSC(-) group in the mean maximum stress at 8 weeks and 12 weeks and the linear stiffness at 12

weeks. ADSC: adipose-derived stem cell